arXiv:1409.0149v1 [cond-mat.stat-mech] 30 Aug 2014

Exact results for a simple epidemic model on a directed network: Explorations of a system in a non-equilibrium steady state.

Maxim S. Shkarayev[1] and R. K. P. Zia[1,2]
[1] *Department of Physics & Astronomy, Iowa State University, Ames, IA, 50011*
[2] *Physics Department, Virginia Polytechnic Institute and State University, Blacksburg, VA, 24061*

Motivated by fundamental issues in non-equilibrium statistical mechanics (NESM), we study the venerable susceptible-infected (SIS) model of disease spreading in an idealized, simple setting. Using Monte Carlo and analytic techniques, we consider a fully connected, uni-directional network of odd number of nodes, each having an equal number of in- and out-degrees. With the standard SIS dynamics at high infection rates, this system settles into an active non-equilibrium steady state. We find the exact probability distribution and explore its implications for NESM, such as the presence of persistent probability currents.

I. INTRODUCTION

Nearly all interesting phenomena around us are non-equilibrium stochastic processes, from all forms of living organisms to the life-sustaining atmosphere and sun. Yet, very little is understood about non-equilibrium statistical systems, especially in comparison to the highly successful Boltzmann-Gibbs framework for systems in thermal equilibrium. Of course, the most important distinction between the two is that, for the latter, once the energy functional (Hamiltonian $\mathcal{H}$) of the system and the properties of the reservoirs (e.g., temperature T, chemical potential μ) are specified, the time-independent microscopic probability distribution, P^*, is known (e.g., a Boltzmann factor, $P^* \propto e^{-\mathcal{H}/k_B T}$). Furthermore, if time-dependent behavior is to be modeled for such systems, a stochastic dynamics can be readily written down, following the rule of detailed balance. One physical consequence for such equilibrium states is that there are no *net* exchanges (e.g., of energy, particles) between the system and its reservoirs. By contrast, we may wish to describe a system in contact with many reservoirs so that, even when it is in a steady (stationary) state, non-trivial net exchanges of various quantities exist. In other words, there are typically net fluxes *through* such systems, as they settle into non-equilibrium steady states (NESS). No one doubts that the existence of our ecosystem depends crucially on such a steady flux of radiant energy, from the sun and to the outer-space. Now, to describe such systems, we must use dynamical rules which violate detailed balance or time-reversal. Then, we face many serious challenges, perhaps the simplest being the following. Given a set of detailed balance violating, stochastic rules of evolution, the system will settle into a NESS; but what is the associated stationary probability distribution, P^*? In addition, it is not surprising that, in analogy with magnetostatics, there will be non-trivial steady (probability) currents, K^*, with which the average net fluxes of observables can be computed [1, 2]. Although a method for constructing P^* and K^* is known [3, 4], it is formal and quite cumbersome. As a result, computing observables with them is hopelessly difficult, while the physics behind these expressions is far from discernible. In particular, there are very few systems for which analytic forms for P^* and K^* are known explicitly. In this context, we study simple model systems – motivated primarily by natural phenomena – which settle into non-trivial NESS, with the goal of gaining some insight into the issues presented above.

In this paper, we consider the venerable SIS model of epidemics [5–8], in which an individual of a population can be in an infected (I) or a susceptible (S) state. While an I spontaneously recovers with some rate, an S can become infected, depending on its connectivity to others and their conditions. If the ratio of infection-to-recovery rates is high enough, a finite fraction of the population are I's, an 'epidemic' is present, and the system is said to be in an 'active' state. In the simplest model, as soon as all I's have recovered, there will be no further evolution, a state labeled as 'inactive.' Of course in reality, spontaneous reinfections (i.e., not due to another I) do occur and the inactive state may be characterized as having a vanishingly small fraction of I's on the average. For public health organizations, the transition between inactive and active states is clearly of major concern. Our interest here is more theoretical, namely, when is an active state a NESS and what are its novel characteristics. In particular, in most model studies, τ_j^i, the probability an infected individual i can affect a susceptible j, is the same as τ_i^j. In reality, infection rates are typically asymmetric (due to, e.g., inherently different immune systems or different habits of personal hygiene), leading us to expect the active states to be NESS. While an undirected graph is adequate for describing the network in the symmetric case, digraphs (i.e., directed graphs) will be needed for a system with $\tau_j^i \neq \tau_i^j$. Our goal here is to explore systems which not only lead to prominently observable effects of detailed balance violation, but also are on the same footing as models obeying detailed balance. These models allow us to construct quantitative and meaningful comparisons between equilibrium and non-equilibrium stationary states. As will be shown, it is remarkable (and fortunate) that we are able to find the explicit analytic forms for P^* and K^*, for an NESS of a well-mixed SIS system with asymmetric infection probabilities, deep in the active phase.

The rest of this paper is organized as follows. In the next section, we present a detail description of the model. Section III will be devoted to the master equation governing the evolution of the probability distribution and a discussion of the role of detailed balance in the dynamics. The exact, microscopic stationary probability distribution and the associated steady currents are provided in a following section. The observable consequences of the underlying persistent currents are explored, with the introduction of a novel macroscopic quantity. After a section on simulation results, we conclude with a summary and outlook. Some technical details are provided in Appendices.

II. MODEL SPECIFICATIONS

We consider the simplest of SIS models [5–8] on fully connected networks of N nodes, evolving stochastically according to the following rules. For reasons to be made clear, we restrict ourselves to odd N $(= 2\ell + 1)$. A node, labeled by i $(= 1, ..., N)$, can be found in one of two states: I or S, infected with or susceptible to a disease, respectively. We specify a configuration (microstate) of the system by $\vec{m}$, (a vector) with entries $m_i = 0$ or 1, when node i is susceptible or infected, respectively. Thus,

$$n\left(\vec{m}\right) \equiv \Sigma_i m_i \tag{1}$$

is the number of infected individuals in microstate $\vec{m}$. Now, configuration space consists of the vertices of a unit cube in N dimensions, while the evolution of our system corresponds to moving from vertex to vertex, only along an edge of this cube. Specifically, the changes occur at discrete time steps, with exactly one event taking place: Either an infected node becomes susceptible, or vice versa. In the language of a kinetic Ising model, these moves correspond to Glauber spin-flip dynamics [9]. Note that our system will always change its state in a step, though the ratio of recovery to infected processes differ in general. Though such a rule seems artificial, it is in the spirit of the well-established Gillespie algorithm in Monte Carlo simulations [10]. When performing computer simulations, taking N steps is referred to as a sweep or a Monte Carlo step (MCS), in which period every node has, on the average, one chance to change its state.

In our model, the recovery process occurs with probability proportional to $r > 0$. Meanwhile, an infected node j can transmit the disease to a susceptible node i with probability proportional to τ_i^j, where the following class of τ_i^j's is considered. Since we do not allow a node to infect itself, we impose $\tau_i^i \equiv 0$. As we wish to consider possibly *asymmetric* infection probabilities $\tau_i^j \neq \tau_j^i$, a convenient way to encode this information is (for $i \neq j$)

$$\tau_i^j = \theta\left(1 + \sigma a_i^j\right), \tag{2}$$

where θ controls the overall rate of infection, σ is a parameter in the interval $[0, 1]$, and a_i^j is a skew-symmetric matrix with elements ± 1. The advantage of the form (2) is that the symmetric and *antisymmetric* aspects of the infection rates are shown explicitly, controlled by θ and $\theta\sigma$, respectively. Thus, if $\tau_i^j = 0$ (i cannot be infected by j), then i can infect j with probability 2θ. Furthermore, σ allows us to tune continuously, from an ordinary SIS model to a network with *maximally asymmetric* infection rates.

Given that N is odd, we can impose $\sum_j a_i^j = 0$, a condition which means that, for $\sigma = 1$, each node will have precisely ℓ in- and out-degrees. In other words, in this special network, each individual can be infected by half of the (rest of the) population and *immune* to the other half. From the form of (2) and $\Sigma_j a_i^j = 0$, it may be argued that the 'average rate' for an individual to be infected is controlled only by θ, so that it is meaningful for us to compare the epidemics levels in networks with different σ's.

Obviously, for $\sigma = 0$, the infection rate are symmetric and uniform, representing the venerable 'well-mixed' SIS model [8]. In the large N limit, this should have vanishingly small fluctuations, and, with no spatial structure, it can be well described by deterministic the rate equation [8]: $dn/dt = -rn + \theta n(N - n)$. As $t \to \infty$, $n\left(t\right)$ will settle into one of two fixed points (n^*): an 'inactive' state ($n^* = 0$), if the infection rate is too low, or an 'active' one with $n^* = N - r/\theta$. The transition occurs at critical ratio $\left(\theta/r\right)_c = 1/N$. There is also much known about such a model on other networks, e.g., those corresponding to populations with spatial structure [11–14].

As it stands, the unique stationary state in the stochastic version is an absorbing state ($\vec{m} = \vec{0}$). For large/small infection/recovery rates, this state is rarely reached and the active state is referred to as quasistationary. We choose a different rule, so that a non-trivial, active state exists as genuinely stationary, namely, by infecting a randomly chosen node whenever the system arrives at $\vec{m} = \vec{0}$. While such a rule will affect the precise determination of the critical parameters for the transition between inactive to active states, it should not play a serious role for systems far in the active state. Should we extend our studies to the critical region, we can always modify this rule to reinfect this state with an arbitrarily small probability.

Let us emphasize that the model presented here is highly specialized, designed to highlight the differences between equilibrium states and NESS, rather than to describe a realistic population. Neverthless, our main result – the presence of cyclic behavior and its quantitative characterization – is expected to prevail in all epidemics, even though these effects are not likely to be dominant.

III. MASTER EQUATION AND DETAILED BALANCE

The full stochastic process specified above is described by a master equation for $P\left(\vec{m}, t\right)$, the probability for find-

ing our system in microstate $\vec{m}$, t steps from some initial configuration. (Since our focus will be the stationary state, reached after very long times, the initial state is irrelevant and will not be explicitly shown here.) In general, the master equation reads

$$P\left(\vec{m},t+1\right)=\sum_{\vec{m}'}R\left(\vec{m}\leftarrow\vec{m}'\right)P\left(\vec{m}',t\right), \tag{3}$$

where R represents the transition probability, to go from $\vec{m}'$ to $\vec{m}$. In our model, these $\vec{m}$'s differ by only one entry (e.g., $m_i'=1-m_i$), so that we can simplify the above to:

$$\begin{aligned}&P\left(m_1,...,m_N,t+1\right)=\\&\sum_i\Omega_i\left(\vec{m}'\right)P\left(m_1,...,1-m_i,....m_N,t\right),\end{aligned} \tag{4}$$

where Ω are the transition probabilities spelled out above. To find the explicit expressions, consider first S to I transitions. For simplicity, we define our model [24] by letting

$$\gamma_i\left(\vec{m}\right)\equiv\sum_j\tau_i^jm_j. \tag{5}$$

be the rate the node i in $\vec{m}$ becomes infected. Here, the m_j insures that j is infected, while τ_i^j embodies both the infection probability and the connectivity between i and j. Substituting (2), we see that

$$\gamma_i\left(\vec{m}\right)=\theta\left[n\left(\vec{m}\right)+\sigma\kappa_i\left(\vec{m}\right)\right], \tag{6}$$

where

$$\kappa_i\left(\vec{m}\right)\equiv\sum_ja_i^jm_j \tag{7}$$

represents an *excess* of the infected individuals who can affect i, over those which cannot do so. On the average, κ would be zero, as a_i^j assigns $+1$ to infected individuals with a link directed to i and -1 to ones direct away from i. Thus, the total rate for *any* susceptible individual in $\vec{m}$ to be infected is (proportional to) the sum

$$\begin{aligned}&\sum_i\left(1-m_i\right)\gamma_i\left(\vec{m}\right)=\theta\sum_{ij}\left(1-m_i\right)\left(1+\sigma a_i^j\right)m_j\\&=n\left(\vec{m}\right)\left[N-n\left(\vec{m}\right)\right]\theta,\end{aligned} \tag{8}$$

where the last equality arises from $a_i^j=-a_j^i$ and $\Sigma_ia_i^j=0$. The significance of this class of asymmetric networks is revealed: The *total* rate of infection does not depend on the details of the digraph (i.e., a_j^i).

For I to S transitions, since each of the n infected nodes can recover independently, the total recovery rate is (proportional to) $rn\left(\vec{m}\right)$. These results provide us with the normalization factor

$$\rho\left(\vec{m}\right)=\frac{1}{n\left(\vec{m}\right)r+n\left(\vec{m}\right)\left[N-n\left(\vec{m}\right)\right]\theta}. \tag{9}$$

Note that this factor depends on $\vec{m}$ only through n, the total number of infected, rather than the details of each individual. Thus, whenever there is no confusion, we will use the simpler notation

$$\rho_n=\frac{1}{nr+n\left(N-n\right)\theta}. \tag{10}$$

Of course, this expression is singular for $\vec{m}=0$, a special case for which $\Omega_i\left(\vec{0}\right)$ is simply $1/N$.

With these forms, $\Omega_i\left(\vec{m}\right)$ is explicitly $\rho\left(\vec{m}\right)\left[m_ir+\left(1-m_i\right)\gamma_i\left(\vec{m}\right)\right]$, for $\vec{m}\neq0$. Since m can be either 0 or 1, Ω is given by one or the other term here. Note that, for the fully infected state, Ω_i reduces to $\rho_Nr=1/N$ for all i, which is completely consistent with our expectations. Inserting these Ω's into Eqn. (4), we have the full master equation. One subtlety we should emphasize is that, in Equation (4) the argument in Ω_i is $\vec{m}'$, which is $\vec{m}$ *except* for entry i, while their n's differs by unity. Thus, it is worthwhile writing the master equation explicitly

$$\begin{aligned}&P\left(m_1,...,m_N,t+1\right)=\\&=\sum_i\left\{\rho_{n+1}\left(1-m_i\right)r+\rho_{n-1}m_i\gamma_i\left(\vec{m}'\right)\right\}\times\\&\times P\left(m_1,...,1-m_i,....m_N,t\right),\end{aligned} \tag{11}$$

where $n=n\left(\vec{m}\right)\in[2,N-1]$. Note that the two terms in $\{...\}$ correspond to recovery and infection, respectively. Of course, these terms must be suitably modified for $n=1$ and N.

Given a set of transition probabilities, it is simple to see if they obey detailed balance using the Kolmogorov criterion [15]. Consider a closed loop involving L configurations, $\vec{m}^{(1)}\rightarrow\vec{m}^{(2)}\rightarrow\ldots\rightarrow\vec{m}^{(L)}\rightarrow\vec{m}^{(1)}$, as well as the product

$$R\left(\vec{m}^{(1)}\leftarrow\vec{m}^{(L)}\right)\ldots R\left(\vec{m}^{(3)}\leftarrow\vec{m}^{(2)}\right)R\left(\vec{m}^{(2)}\leftarrow\vec{m}^{(1)}\right)$$

along it and the product

$$R\left(\vec{m}^{(1)}\leftarrow\vec{m}^{(2)}\right)\ldots R\left(\vec{m}^{(L-1)}\leftarrow\vec{m}^{(L)}\right)R\left(\vec{m}^{(L)}\leftarrow\vec{m}^{(1)}\right)$$

for traversing the loop in reverse. If and only if these products are equal for *all* loops, detailed balance is satisfied. Then, the stationary distribution can be thought of as one in thermal equilibrium, with no net probability currents anywhere. In Appendix A, we provide some details which show that, in general, detailed balance is violated if $\sigma>0$. It is hardly surprising that an SIS model on a complete, undirected graph settles into an equilibrium state (with zero net currents, as in electrostatics). By contrast, systems with $\sigma>0$ will evolve towards *non*-equilibrium steady states with persistent currents (as in magnetostatics) [1]. One of the goals of this study is to show, both analytically and in Monte Carlo simulations, the existence of these currents and their implications for observables. But first, let us find the stationary distribution.

IV. EXACT STEADY STATE DISTRIBUTION AND PERSISTENT PROBABILITY CURRENTS

It is well known that the equation (3), with the transition probabilities given here, will evolve P to a stationary state, which we denote by $P^*(\vec{m})$. If the dynamics satisfies detailed balance, then finding this P^* is a trivial process. Otherwise, though there is a systematic method to construct P^* [3], this route is prohibitively cumbersome and, typically, finding an explicit P^* is essentially impossible. Nevertheless, under a few special circumstance, such P^*'s have been found. The simplest example is biased diffusion on a ring. Introduced as the asymmetric exclusion process [16–18], $P^* \propto 1$ was known long ago [19]. Here, we are able to find a non-trivial P^*, based on an Ansatz inspired by simulation results. Since our dynamics is clearly ergodic, this P^* is unique, so it is *the* stationary distribution.

A. P^* for the undirected network

Before we present the general result, let us recapitulate well-known results, for the reader's convenience, in the simple SIS model on a complete and undirected network ($\sigma = 0$). Of course, due to the reinfection of the inactive state, our results for P^* are slightly different from the distribution for a quasistationary state.

Since this dynamics satisfies detailed balance, we simply start with an unknown $P^*\left(\vec{0}\right)$ and obtain the rest by repeated use of $R(\vec{m} \leftarrow \vec{m}')\, P^*(\vec{m}') = R(\vec{m}' \leftarrow \vec{m})\, P^*(\vec{m})$. Note that this condition reflects the simple balance between the infection and recovery rates for any *single* individual. For a complete, undirected graph, it is clear that $R(\vec{m}' \leftarrow \vec{m})$ depends only on n. Therefore, $P^*(\vec{m})$ is also a function of $n(\vec{m})$ only and so, we write:

$$P^*(\vec{m}) = P_n. \tag{12}$$

In terms of these, the balance of the rates for a single node (i.e., $\rho_n r P_n$ for recovery and $\rho_{n-1}(n-1)\theta P_{n-1}$ for infection) leads to

$$\rho_n r P_n = \rho_{n-1}(n-1)\theta P_{n-1}. \tag{13}$$

This recursion allows us to express the P_n's in terms of P_0, starting with the special case $\rho_1 r P_1 = P_0/N$. Thus,

$$\begin{aligned} P_n &= (n-1)!\alpha^{n-1}\frac{P_0}{\rho_n r N} = \\ &= \left\{\phi_n \alpha^{n-1}(n-1)! + (1-\phi_n)\alpha^n n!\right\} P_0 \end{aligned} \tag{14}$$

for $n \geq 1$, where

$$\phi_n \equiv n/N \tag{15}$$

is the fraction (of the infected in $\vec{m}$), and

$$\alpha \equiv \theta/r \tag{16}$$

is the ratio of the rates (which is clearly the only quantity of significance here). We remark that the various factors in Eqn. (14) lend themselves to intuitive interpretations: relative weights for the infected and susceptible factions, cumulative factors for infection (α^n), and combinatorics.

Finally, the unknown P_0 can be fixed by imposing normalization, namely, $1 = \sum_{\vec{m}} P^*(\vec{m}) = \sum_{n=0}^{N} \binom{N}{n} P_n$ (to account for the $\binom{N}{n}$ microstates $\vec{m}$ for a specific n). Thus,

$$\begin{aligned} \frac{1}{P_0} = 1 &+ \sum_{n=1}^{N} \binom{N}{n} \frac{n!\alpha^{n-1}}{N} + \\ &+ \sum_{n=1}^{N} \binom{N}{n} \frac{n!\alpha^n}{N}(N-n). \end{aligned} \tag{17}$$

In Appendix B, we show P_0 can be expressed compactly as

$$P_0 = \frac{e^{-1/\alpha}}{2\alpha^{N-1}\Gamma(N, 1/\alpha)}. \tag{18}$$

where Γ is an upper incomplete gamma function. Note that it may appear counter-intuitive that, by setting the infection rate θ to zero, $P_0 = 1/2$ is less than unity. This result is merely an artifact of our special rule for reinfecting the absorbing state as soon as it is reached. If this rule is modified appropriately, P_0 can be made arbitrarily close to unity.

B. P^* for an asymmetric network

Let us turn to the general $\sigma > 0$ case, in which i can infect j with a rate different from the opposite situation. Though there is no *a priori* reason to expect $P^*(\vec{m})$ to depend only on $n(\vec{m})$, we are inspired by simulation results (shown below) indicating that this property persists. Thus, we attempt to find a stationary solution to Eqn. (4,11) with $\sigma > 0$ by using an *Ansatz*: $P^*(\vec{m}) = \tilde{P}_n$. Substituting this Ansatz into

$$\begin{aligned} &\tilde{P}_n = P^*(m_1, ..., m_N) = \\ &\sum_i \left\{\rho_{n+1}(1-m_i)\, r + \rho_{n-1} m_i \gamma_i(\vec{m}')\right\} \times \\ &\times P^*(m_1, ..., 1-m_i, ...m_N), \end{aligned} \tag{19}$$

we see that the right hand side reduces to the following two terms:

$$\sum_i \rho_{n+1}(1-m_i)\, r\tilde{P}_{n+1} + \sum_i \rho_{n-1} m_i \gamma_i(\vec{m}')\, \tilde{P}_{n-1}. \tag{20}$$

Since $\tilde{P}_{n+1}$ does not depend on i, the first sum leads to $\rho_{n+1}[N-n]\, r\tilde{P}_{n+1}$. To carry out the sum in the second requires a little more care, since $\vec{m}'$ stands for $(m_1, ..., 1-m_i, ...m_N)$, with $n(\vec{m}') = n-1$. Thus,

$$\sum_i m_i \gamma_i(\vec{m}') = \theta \sum_i m_i \left[n - 1 + \sigma \Sigma_j a_i^j m_j\right] = n(n-1)\theta \tag{21}$$

is *independent* of σ, while (19) becomes

$$\tilde{P}_n = \rho_{n+1}\left[N-n\right] r\tilde{P}_{n+1} + \rho_{n-1} n\left(n-1\right)\theta\tilde{P}_{n-1}, \quad (22)$$

for $n \geq 2$. Since our reinfection rule for $\vec{m}=0$ is special, we need to supplement these with

$$\tilde{P}_1 = \rho_2\left[N-1\right] r\tilde{P}_2 + \left(1/N\right)\tilde{P}_0. \quad (23)$$

A solution to this set of equations can be found directly; however, given that they are independent of σ, it behooves us to consider $\tilde{P}_n = P_n$. Recalling $\rho_n r N = 1/\left\{\phi_n + \left(1-\phi_n\right)n\alpha\right\}$, it is straightforward to check that

$$\rho_{n+1}\left[N-n\right] r\frac{P_{n+1}}{P_n} = \frac{\left(1-\phi_n\right)\alpha n}{\phi_n + \left(1-\phi_n\right)n\alpha} \quad (24)$$

$$\rho_{n-1} n\left(n-1\right)\theta\frac{P_{n-1}}{P_n} = \frac{\phi_n}{\phi_n + \left(1-\phi_n\right)n\alpha}, \quad (25)$$

and so, P_n indeed satisfies Eqn. (22). Thus, our expectation, that expression (14) is the stationary distribution $P^*\left(\vec{m}\right)$ for *any* σ, is verified.

C. Persistent probability currents and their consequences

Since Eqn. (3) is a continuity equation for the probability density, it is natural to regard the right hand side as a sum over probability currents. In our case, the *net* current from microstate $\vec{m}'$ to $\vec{m}$ (over the single time step $t \to t+1$) can be identified as

$$\begin{aligned} &K\left(\vec{m}' \to \vec{m}, t\right) = \\ &= R\left(\vec{m} \leftarrow \vec{m}'\right) P\left(\vec{m}', t\right) - R\left(\vec{m}' \leftarrow \vec{m}\right) P\left(\vec{m}, t\right). \end{aligned} \quad (26)$$

In the steady state, we denote this quantity by

$$\begin{aligned} &K^*\left(\vec{m}' \to \vec{m}\right) = \\ &= R\left(\vec{m} \leftarrow \vec{m}'\right) P^*\left(\vec{m}'\right) - R\left(\vec{m}' \leftarrow \vec{m}\right) P^*\left(\vec{m}\right). \end{aligned} \quad (27)$$

Thus, if the underlying dynamics obeys detailed balance, K^* vanishes everywhere. Otherwise, there must be non-trivial K^*'s, which we refer to as *persistent currents*. Since only one individual can change state, a current is naturally associated with an edge of the N-cube. For example, for $m_i = 1 \leftrightarrow m_i' = 0$, this current is

$$K^*\left(\vec{m}' \to \vec{m}\right) = \rho_n \gamma_i\left(\vec{m}'\right) P_n - \rho_{n+1} r P_{n+1}, \quad (28)$$

where n stands for $n\left(\vec{m}'\right)$. Using Eqns. (6,13), we have

$$\begin{aligned} &K^*\left(\vec{m}' \to \vec{m}\right) = \rho_n\theta\left[n + \sigma\kappa_i\left(\vec{m}\right)\right] P_n - \rho_{n+1} r P_{n+1} = \\ &= \sigma\kappa_i\left(\vec{m}'\right)\rho_n\theta P_n, \end{aligned} \quad (29)$$

(apart from the cases near $n = 0, N$). From (7), we see that $\kappa_i\left(\vec{m}\right) = \kappa_i\left(\vec{m}'\right)$ since both are independent of m_i. The final expression is

$$K^*\left(\vec{m}' \to \vec{m}\right) = \left[\sigma\kappa_i\left(\vec{m}\right)\right]\alpha^n\left(n-1\right)! P_0/N, \quad (30)$$

showing explicitly that it vanishes with the product of the asymmetry strength (σ) and the 'excess' (κ_i) of infected individuals connected to i.

Such microscopic currents (on a discrete space) are analogous to current densities in electrodynamics and hydrodynamics. In a stationary state, the divergence free condition implies that the K*'s must form closed loops. In analogy with fluid dynamics, we may refer to the 'curl' of such (probability) currents as 'probability vorticity,' ω. In our discrete configuration space, such an ω should be associated with a face of the cube (plaquette) and defined as the *sum* of the currents around the face ($\sim \oint \vec{j}\cdot d\vec{\ell}$ in hydrodynamics). Let us consider the vorticity around the i-j plaquette (i.e., A1). The four K^*'s involved starts with the state $\{m_i, m_j, \hat{m}\} = \{0, 0, \hat{m}\}$, where $\hat{m}$ denotes $m_{k\neq i,j}$, with ν infected individuals. With details shown in Appendix C, this current loop sums to

$$\begin{aligned} \omega^*_{ij} &= \left(P_0/N\right)\alpha^\nu\left(\nu-1\right)!\times \\ &\times\left[\left(\alpha\nu - 1\right)\sum_{k\neq i,j}\left(a^k_j - a^k_i\right)m_k + 2a^i_j\right]. \end{aligned} \quad (31)$$

If we sum over all possible $\hat{m}$'s, all details of the rest of the system (such as ν) disappear and the result can be regarded as a 'coarse-grained' vorticity:

$$\omega^*_{ij|cg} \equiv \sum_{\{\hat{m}\}}\omega^*_{ij}. \quad (32)$$

Not surprisingly, such a vorticity is proportional to the key ingredients of asymmetry, σa^i_j:

$$\omega^*_{ij|cg} = \hat{\omega} a^i_j, \quad (33)$$

where

$$\hat{\omega} = \frac{\sigma}{N S_{N-1}\left(\alpha\right)}\left(\frac{S_{N-2}(\alpha)-1}{N-2} + \alpha S_{N-3}(\alpha)\right) \quad (34)$$

depends on, apart from σ, only the basic control parameters N and α. Here, $S_N(\alpha)$ is defined in Eqn. (B1).

While the analysis above is valuable at the microscopic level, the behavior of macroscopic observables are often more interesting, in that they exemplify collective behavior in a statistical mechanical system. For example, though the microscopic distribution of an Ising model is trivially analytic, the properties of the total mangetisation (analog of n here) signal phase transitions and display highly non-trivial singularities. In this spirit, we turn to macroscopic observables which reveal the presence of probability current loops. In classical mechanics, mass currents (and loops) are ubiquitous. For example, in rotation of rigid bodies, these currents are more commonly characterized by the total angular momentum $\vec{L} = \int \vec{r}\times\vec{v}\rho\left(\vec{r}\right)dr$. Exploiting the notion that $\rho\vec{v}$ represents the mass current, we will introduce the analog of $\vec{L}$ here, in the context of the simplest of examples.

Consider two subgroups of our population, labeled by $g = 1, 2$. For convenience, let them have equal size: $N_1 = N_2$. An obvious macroscopic variable is the pair (n_1, n_2), the number of infected individuals in each. From the microscopic $P(\vec{m}, t)$, a distribution in the $N_1 \times N_1$ square of integers can be defined

$$\mathcal{P}(n_1, n_2, t) \equiv \sum_{\{\vec{m}\}} \delta\left(n_1 - \sum_{i\in[1]} m_i\right) \times \times \delta\left(n_2 - \sum_{i\in[2]} m_i\right) P(\vec{m}, t), \tag{35}$$

where $i \in [g]$ means the individuals in subgroup g. After long times, this settles into a stationary distribution $\mathcal{P}^*(n_1, n_2)$. Since $P^*(\vec{m})$ is independent of the details of $\vec{m}$, $\mathcal{P}^*(n_1, n_2)$ can be computed readily. Deep in the active phase, we expect it to be quite ordinary, well approximated by a Gaussian peaked around $(N_1, N_2)(1-1/\alpha N)$. On the other hand, K^* does depend on the details of the partition, through a_j^i. The analogy between K^* and the mass current leads us to consider a 'probability angular momentum.' Associated with the stochastic time trace of (n_1, n_2) in the $N_1 \times N_1$ square, such an angular momentum has only one component, which we will denote by $\mathcal{L}$. Furthermore, since our model is defined by discrete time steps, the classical velocity in $\vec{L}$ will be replaced by the difference $(n_1' - n_1, n_2' - n_2)$, where (n_1', n_2') are the numbers one step later. Thus,

$$\mathcal{L} \equiv (n_1, n_2) \times (n_1' - n_1, n_2' - n_2) = n_1 n_2' - n_2 n_1', \tag{36}$$

while

$$\langle \mathcal{L} \rangle = \sum_{\{\vec{m}, \vec{m}'\}} (n_1 n_2' - n_2 n_1') K^*(\vec{m} \to \vec{m}'). \tag{37}$$

Indeed, we can venture further, using finite time differences instead of single steps:

$$\langle \mathcal{L}_t \rangle \equiv \sum_{\{\vec{m}, \vec{m}'\}} (n_1 n_2' - n_2 n_1') Q^*(\vec{m}', t; \vec{m}, 0), \tag{38}$$

where $Q^*(\vec{m}', t; \vec{m}, 0)$ is the joint probability for finding the system in microstate $\vec{m}$ at time 0 and in $\vec{m}'$ t steps later (in the NESS). Formally, Q^* is given by iterating Equation (3) t times, while $\langle \mathcal{L}_t \rangle$ is recognizable as the antisymmetric part of a (certain combination of a) two point, time-dependent correlations, i.e., $\langle m_i(t)\, m_j(0) \rangle$ in other common notations. In practice, writing down these expressions is facile, but computing them analytically is non-trivial and beyond the scope of this paper. Instead, we will turn to Monte Carlo simulations to study their properties.

V. SIMULATION STUDIES

Although we have some key exact results, finding expectations of macroscopic quantities is not feasible in general. For example, though Lenz had the explicit microscopic distribution for an Ising model in the 20's, two decades passed before a ferromagnetic transition is shown to exist (in two dimensions). In our SIS model, despite both P^* and K^* being explicitly known, many observables – especially those associated with non-equilibrium statistical mechanics – cannot be computed exactly. Though we expect these quantities can be well described by mean-field approximations, we will rely on computer simulations here.

Specifically, we will focus on two extreme cases of the system: $\sigma = 0$ and 1, corresponding to an undirected all-to-all network and a directed network in which every node has ℓ in- and out-degrees, respectively. Since the connectivity differs by a factor of 2, while the individual infection probabilities differ by 1/2, the overall characteristics of the epidemic are indistinguishable and it is meaningful to compare the two systems. In particular, as we have shown in Section III, the former settles into an 'equilibrium' system while the latter becomes a NESS. In the rest of the section we show simulation results, using $\alpha(N-1) = 1.6$ (corresponding to an active epidemic, with a level of $\sim 40\%$), which highlight their similarities and differences. Before we discuss studies with sizable N's, let us present P^* and K^* for a very small system, just to verify that simulations indeed generate exact results.

A. Results for the microscopic P^* and K^* in a system with $N = 7$

If we wish to compare the two approaches for these microscopic distributions, we are severely restricted, given that there are 2^N configurations. While $N = 3$ is obviously trivial, we also find a special aspect to all $N = 5$ systems satisfying the $\Sigma_j a_i^j = 0$ constraint. Namely, the nodes can always be permuted so that their connectivities are identical and all graphs are circulant. At $N = 7$, it is possible to construct several distinct classes of networks with $\Sigma_j a_i^j = 0$. In Appendix D, we provide the full algorithm for constructing a general, random network of this type. Returning to our particular $N = 7$ system, we label the 128 configurations, $\{m_1, ..., m_7\}$, by its binary code (e.g., $\{1, 0, 1, 0, 0, 1, 0\} \Longrightarrow k \equiv \sum_{i=1}^{N} m_i 2^{i-1} = 37$). The specific a_i^j chosen is displayed in Figure 3(c) and we perform Monte Carlo simulations with the rules specified in Section II. Typically, we discard the first 10^3 MCS to ensure the system has settled into stationary states. Thereafter, we typically take measurements for the next 10^6 MCS.

First, as shown in Figure 1, simulations confirmed that the microscopic stationary distributions P^* for both systems are (statistically) identical. By contrast, we display in Figures 2(a) and 2(b) the dramatic differences between the two steady state currents, $K^*(\vec{m}' \to \vec{m})$. The units correspond to the fraction of the time the system makes the transition $\vec{m}' \to \vec{m}$ *minus* the fraction of $\vec{m} \to \vec{m}'$.

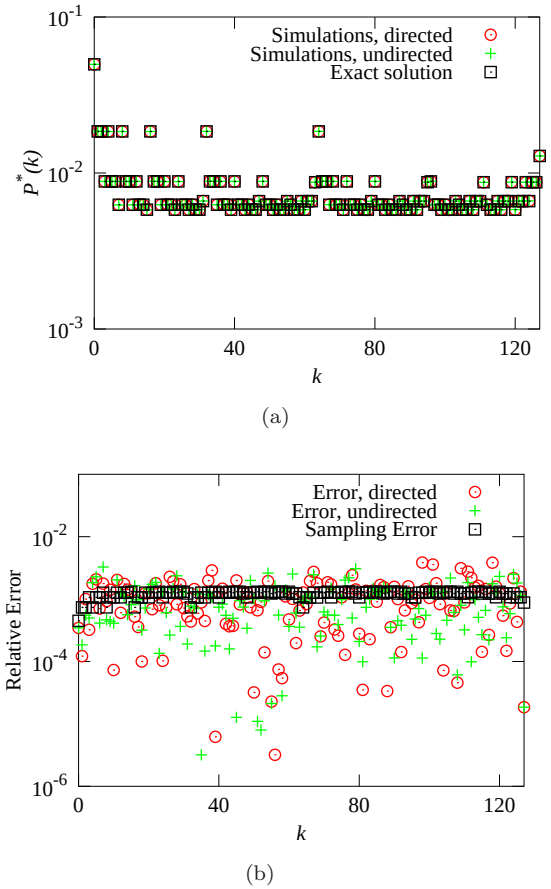

FIG. 1: (Color online) Comparison of the simulation results of the two systems with the exact solution, Eq. (14). There are $N = 7$ nodes in both the directed and undirected systems, set at $r = 1$ and $\theta \approx 0.267$. (a) For each value of k, simulation data for both systems and the exact results coincide. (b) The relative error, $|1 - P^*_{\text{simulations}}(k)/P^*_{\text{exact}}(k)|$, compared with the expected sampling error, $1/\sqrt{f_k}$, f_k being the frequency we observe the system being in microstate k during the run.

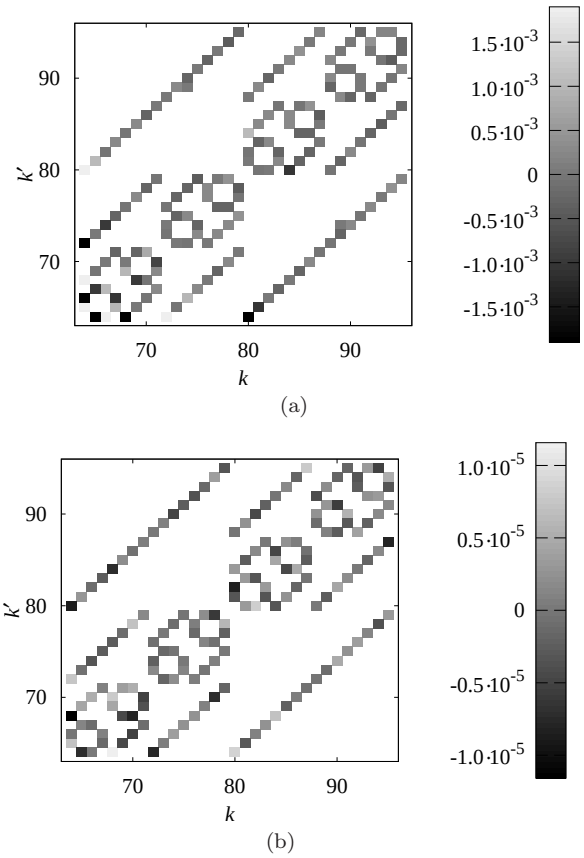

FIG. 2: Probability currents, $K^*(k, k')$, measured in simulations for the (a) directed and (b) undirected systems. Only a portion of all the 128×128 currents are shown. Note the difference in the scales for the two cases.

Since there is no connection between many pairs of $\{\vec{m}\}$'s, we have illustrated the $2^7 \times 2^7$ K^*-'matrix' by showing only a small section: $k, k' \in [64, 95]$. Note that, in the $\sigma = 0$ system, the averages are consistent with zero, while the values shown are more indicative of noise. As typical deviations in a sampling distribution of the Ks, we fully expect these values to decrease with the length of the simulation run. In stark contrast, these averages are clearly non-trivial for the $\sigma \neq 0$ system, as we expect them to approach constants as the run time increases. Not surprisingly, these values are (statistically) the same as those predicted in Equation (30).

Finally, at this microscopic level, we can compare the 21 coarse-grained vorticities, $\omega^*_{ij|cg}$. Similar to those for K^*, Figure 3 shows that simulations confirm the theoretical results (Equations (33), (34)). In particular, the similarity between Figures 3(a) and 3(c) is unmistakably clear.

B. Simulation results for $N = O(100)$

Lastly, we turn to more macroscopic quantities, such as $\mathcal{L}$. Intuitively, we expect that the effects of detailed balance violation will be maximal if *all* the links between the two subgroups are oriented in the same direction. Due to the constraint $\Sigma\, a^j_i = 0$, such subgroups cannot be too large. We first performed simulations with $N = 81$, $\alpha = 0.02$, $\sigma = 1$, and $N_g = 20$ with all cross links between the subgroups directed from 1 to 2. After discarding 10^6 steps ($\sim 10^4$ MCS), we collected $n_{1,2}$ for $T \equiv 10^8$ steps and constructed the time average

$$\frac{1}{T-t}\sum_{\tau=0}^{T-t}\left[n_1(\tau)\, n_2(\tau+t) - n_2(\tau)\, n_1(\tau+t)\right] \qquad (39)$$

as a measure for $\langle \mathcal{L}_t \rangle$. As a comparison, we also obtained similar results for the undirected case ($\sigma = 0$). As in the $N = 7$ simulations, Figure 4 shows the dramatic difference in $\langle \mathcal{L}_t \rangle$ between the two models. The most prominent feature is that $\langle \mathcal{L}_t \rangle$ is positive. The same intuitive picture offered above for this sign can be restated here. Since the links all direct from 1 to 2, we may expect

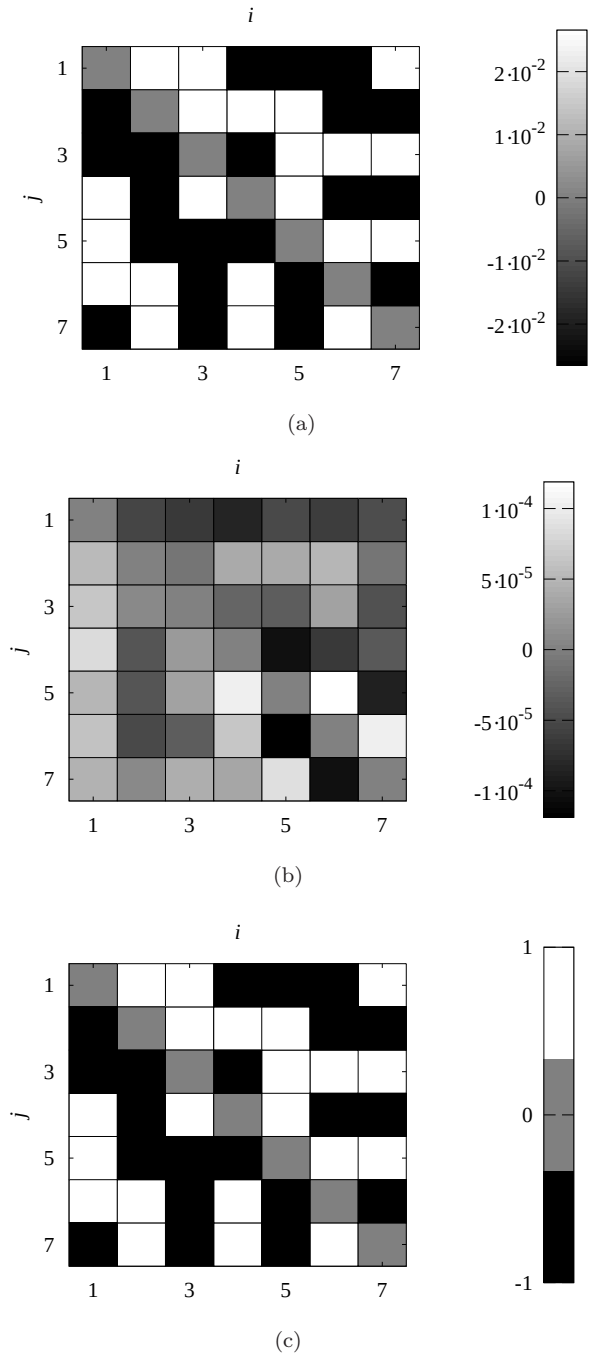

FIG. 3: Coarse-grained vorticity around the i-j plaquette in a directed (a) and an undirected (b) network. (c) Adjacency matrix in our directed network.

that a fluctuation in n_1 (say, increase) will lead, in the next few steps, to more infected individuals in subgroup 2. By contrast, outbreaks in the latter do not affect those in subgroup 1.

At present, we have no quantitative explanation for the other notable feature: the rise and fall of $\langle \mathcal{L}_t \rangle$ as a function of t. Nevertheless, we may consider the following argument. Since the data is plotted against time *steps*, we can reasonably expect that it take $O(N_g)$ steps before correlations associated with the collective behavior of the group is built up. On the other hand, the system is far from being critical, so that we may expect finite correlation times, which would lead to decays at large t. To see if these notions are worth pursuing, we carry out a simple scaling analysis, using $N_g = 10, 20, 80, 100$ in populations with $N = 41, 81, 161, 401$ and correspondingly modified $\alpha = 0.04, 0.02, 0.01, 0.004$. As Figure 4 shows, we find excellent data collapse when $\langle \mathcal{L}_t \rangle / N$ is plotted against t/N (i.e., MCS). The scaling $\langle \mathcal{L}_t \rangle \sim N$ can be argued as follows. Though we expect each n_α to scale with N, the quantities which enters into $\mathcal{L}$ are actually deviations from $\langle n_\alpha \rangle$. If we naively assume that the deviations scale as $\sqrt{N}$, then we arrive at $\langle \mathcal{L}_t \rangle \sim N$. Work is in progress on both the simulation and the theoretical fronts, to draw reliable conclusions and to achieve an in-depth understanding of these phenomena.

As a final note, we present relevant data concerning the *fluctuations* in $\mathcal{L}$, since a valid question could be raised concerning the standard deviation associated with the observed averages. To appreciate better such issues, let us first illustrate with one particular case – $N = 81, \alpha = 0.02, t = 40$ (corresponding to the peak in Figure 4), by displaying the full distributions of the observed $\mathcal{L}$'s, $p(\mathcal{L})$, for both the $\sigma = 0$ vs. 1 models. Since $|\mathcal{L}| \leq 20^2$, the range shown here is reasonable. While the two curves in Figure 5(a) are quite broad and give the impression of being indistinguishable, a plot of the asymmetry in Figure 5(b) clearly displays the difference. As a result of this asymmetry, $\langle \mathcal{L}_{40} \rangle \cong 0.512$ in the NESS case. By contrast, it is consistent with zero ($\sim 10^{-4}$) for the undirected network. Quantitatively, the standard deviations for the $\sigma = (0, 1)$ cases are, respectively, approximately $(27.6, 27.8)$, with skewness $\left(10^{-4}, 0.0597\right)$ and kurtosis $(0.704, 0.6961)$. Clearly not Gaussians, these distributions deserve to be studied in further detail. Similarly, there appears to be interesting features in the asymmetry plot. We should pursue them and ask if their origin is merely a chance fluctuation or some systematic intriguing physics.

VI. SUMMARY AND OUTLOOK

We study a simple SIS model of epidemics on a complete graph with infection rates that interpolate between symmetric ($\sigma = 0$) and fully antisymmetric ($\sigma = 1$). In the language of graphs, these correspond to undirected and directed ones, respectively, the latter associated with an antisymmetric (part of the) adjacency matrix a_i^j. To make comparisons between models with different σ meaningful, we impose a restriction: $\Sigma_i \, a_i^j = 0$, i.e., every node has the same number of in- and out-degrees when $\sigma = 1$. With relatively high infection rates (and a small reinfection probability to avoid being trapped in the absorbing state), the system settles into an active state, which is an equilibrium stationary state or a non-equilibrium one, re-

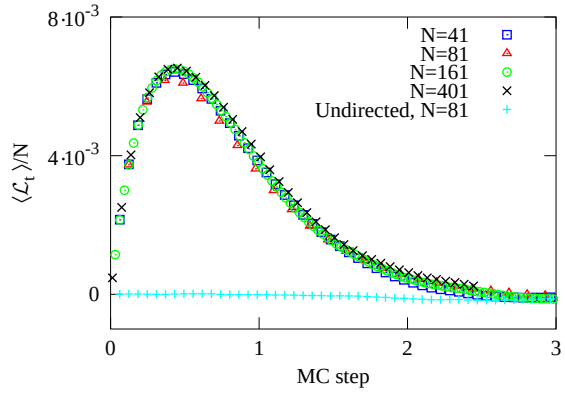

FIG. 4: (Color online) Scaled plot of $\langle \mathcal{L}_t \rangle / N$, showing good data collapse for four cases: $N = 41, 81, 161, 401$. The unit of time here is MCS.

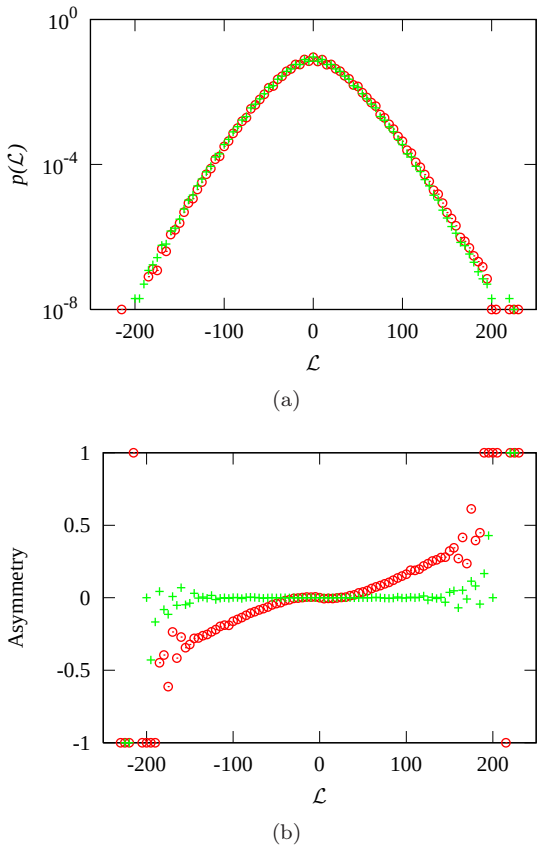

FIG. 5: (Color online) (a) Distributions of $\mathcal{L}$, $p(\mathcal{L})$, obtained from histograms of observed values in a run of 10^8 steps, for the undirected network ($\sigma = 0$, green pluses) and the directed one ($\sigma = 1$, red open circles). (b)Asymmetry in the distributions, defined as $[p(\mathcal{L}) - p(-\mathcal{L})] / [p(\mathcal{L}) + p(-\mathcal{L})]$, highlighting the different behaviors associated with the undirected network ($\sigma = 0$, green pluses) and the directed one ($\sigma = 1$, red open circles).

spectively. Solving the master equation exactly, we find that the stationary distribution, P^*, is *independent* of σ. Such a result is reminiscent of the one in the asymmetric simple exclusion process [19], in which $P^* \propto 1$, regardless of the strength of the bias. Thus, static properties, such as phase transitions, critical behavior and equal time correlations, will also be independent of σ.

On the other hand, the dynamics of a $\sigma > 0$ system violates detailed balance, so that non-vanishing steady (probability) currents will be present. In the stationary state, these must form closed loops, as in mangetostatics. Their consequences will be observable only when dynamic quantities (e.g., unequal time correlations) are measured. At the microscopic level, these current loops form vortices around a plaquette associated with a pair of nodes: (i, j). The vorticities, also found exactly, are proportional to, as expected, σa_i^j. Physically, they correspond to the frequency of cyclic infection-recovery behavior: in $(SS \to SI \to II \to IS \to SS)$ *vs.* the reverse loop. At the macroscopic level, we can consider two groups of individuals and the numbers of the infected: (n_1, n_2). One consequence of non-zero probability currents is that, in general, trajectories in the n_1-n_2 plane are more likely to circulate one way rather than the other. We focus on a particular quantity, $\mathcal{L}$, which is the analog of angular momentum in classical mechanics and being studied in the context of the climate science [20]. Dubbed the 'probability angular momentum,' it is simply the antisymmetric part of an unequal-time correlation between two quantities. Illustrating with a specific example, $\langle n_1(0)\, n_2(t) - n_2(0)\, n_1(t) \rangle$ is found to display interesting properties. Though the qualitative aspects are expected, much of the quantitative features remains to be analyzed.

Naturally, our study here raises many interesting questions, from those related to SIS models to a wider spectrum of systems in non-equilibrium steady states. For our SIS model, we fully expect that, deep in the active phase, the fluctuations and correlations can be well approximated by a linear Langevin equation, leading to Gaussian (but non-equilibrium) distributions [1, 21–23]. The associated currents are well understood [1] and distributions for collective quantities like $p(\mathcal{L})$ can then be computed [20].

Beyond our simple system with all-to-all connections, there are many SIS models, cast in the context of a variety of networks (e.g., square periodic lattice) [11–14]. Further, to model realistic epidemics, SIS is too simplistic. In more complex models, it is also very likely that their evolution violate detailed balance, so that persistent probability currents should be present in those steady (or quasi-stationary) states. We are not aware of any studies on observable consequences of these currents and believe that such pursuits can yield new insights into both cylclic behavior in a quasi-stationary ongoing epidemic and the variety of paths to its extinction. We expect the results presented here to provide some guidance in the search for novel manifestations of probability currents.

In a wider context, since probability currents necessarily persist in NESS [1], the study of their observable manifestations is of some importance. The range of these manifestations in nature is enormous, from convection cells of all varieties and sizes (Raleigh-Benard, Kelvin-Helmholtz) to energy/matter fluxes *through* all living organisms. The relationship between microscopic probability currents and such macroscopic phenomena has been explored in, e.g., [1]. Two intriguing possibilities exist. One is that, under coarse-graining, the effects of these currents become less and less relevant (in the renormalization group sense). There are few investigations on how such renormalization group flows, despite the importance of understanding this class of systems. To study the other possibility – effects surviving coarse-graining – is clearly more urgent, since macroscopic currents are essential for life and ubiquitous in nature. Of course, our distant goal lies far beyond the models of epidemics considered here. It is to develop an overarching framework to characterize such behavior for all stochastic processes which allow the system to settle into non-equilibrium steady states. In such a framework, probability distributions of currents will play a central role, just as the probability distributions of configurations is central to equilibrium statistical mechanics.

Acknowledgments

We acknowledge fruitful discussions with B. Fox-Kemper, D. Mandal, B. Schmittmann, Z. Toroczkai, and J.B. Weiss. This research is supported in part by the US National Science Foundation through grants DMR-1244666 and DOS-1245944.

Appendix A: Detailed Balance and Kolmogorov Criterion

Since all loops in configuration space can be regarded as sums of 'elementary' loops, each winding around a face (plaquette), this criterion can be checked by studying the product of Ω's around an elementary loop. Thus, we consider the sequence

$$(m_i, m_j) = (0,0) \to (1,0) \to (1,1) \to (0,1), \tag{A1}$$

with all other entries $(m_{k\neq i,j})$ held fixed. For simplicity, we use only these two m's as shorthand to stand for the four configurations. Thus, if we define $n_0 \equiv \Sigma_{k\neq i,j} m_k$, and $n_{1,2} = n_0 + 1, 2$, the sequence of $n(\vec{m})$'s and ρ's are

$$n_0 \to n_1 \to n_2 \to n_1 \to n_0, \tag{A2}$$

$$\rho_0 \to \rho_1 \to \rho_2 \to \rho_1 \to \rho_0, \tag{A3}$$

where $\rho_\alpha \equiv 1/\left[n_\alpha \left\{r + \theta\left(N - n_\alpha\right)\right\}\right]$ is just a short hand for ρ_{n_α}. With this notation, the associated product of the transition probabilities is $\Pi \equiv \Omega_i(0,0)\,\Omega_j(1,0)\,\Omega_i(1,1)\,\Omega_j(0,1)$, i.e.,

$$\Pi = \rho_0 \gamma_i(0,0)\,\rho_1 \gamma_j(1,0)\,\rho_2 n_2 r \rho_1 n_1 r, \tag{A4}$$

For the loop in reverse, the product is $\Pi_R \equiv \Omega_i(0,0)\,\Omega_j(0,1)\,\Omega_i(1,1)\,\Omega_j(1,0)$, i.e.,

$$\Pi_R = \rho_0 \gamma_j(0,0)\,\rho_1 \gamma_i(0,1)\,\rho_2 n_2 r \rho_1 n_1 r. \tag{A5}$$

The Kolmogorov criterion, $\Pi \stackrel{?}{=} \Pi_R$, reduces to

$$\gamma_i(0,0)\,\gamma_j(1,0) \stackrel{?}{=} \gamma_j(0,0)\,\gamma_i(0,1). \tag{A6}$$

Using Eqn. (6), this test becomes

$$\begin{aligned} &\left[n_0 + \sigma\kappa_i(0,0)\right]\left[n_1 + \sigma\kappa_j(1,0)\right] \stackrel{?}{=} \\ &\stackrel{?}{=} \left[n_0 + \sigma\kappa_j(0,0)\right]\left[n_1 + \sigma\kappa_i(0,1)\right], \end{aligned} \tag{A7}$$

or

$$\begin{aligned} &\sigma\left\{n_0\left[\kappa_j(1,0) - \kappa_i(0,1)\right] + \right. \\ &\left. + n_1\left[\kappa_i(0,0) - \kappa_j(0,0)\right]\right\} + \\ &+ \sigma^2\left[\kappa_i(0,0)\,\kappa_j(1,0) - \kappa_j(0,0)\,\kappa_i(0,1)\right] \stackrel{?}{=} 0, \end{aligned} \tag{A8}$$

where

$$\begin{aligned} \kappa_i(\mu,\mu') &= \sum_k a_i^k m_k + a_i^j \mu', \\ \kappa_j(\mu,\mu') &= \sum_k a_j^k m_k + a_j^i \mu. \end{aligned} \tag{A9}$$

Clearly, the equality can fail provided $\sigma > 0$ and so, the differences above do not vanish for a general $\vec{m}$. Note however, that it does vanish with σ, which indicates that, not surprisingly, SIS on a complete, undirected graph settles into an equilibrium state.

Appendix B: Normalization Factor

To compute the sum in Eqn. (17), we consider

$$S_N(\alpha) \equiv \sum_{n=0}^{N} \binom{N}{n} n!\alpha^n = \int_0^\infty \mathrm{d}x e^{-x}\left(1+\alpha x\right)^N, \tag{B1}$$

where $n! = \int e^{-x} x^n$ is used and the sum is performed first. Changing the integration variable to $y = x + 1/\alpha$, this becomes

$$\begin{aligned} S_N(\alpha) &= \alpha^N e^{1/\alpha} \int_{1/\alpha}^\infty \mathrm{d}y e^{-y} y^N = \\ &= \alpha^N e^{1/\alpha} \Gamma\left(N+1, 1/\alpha\right), \end{aligned} \tag{B2}$$

where Γ is the upper incomplete gamma function. Thus, (17) can be written as

$$\frac{1}{P_0} = \frac{1}{\alpha N} \sum_{n=1}^{N} \binom{N}{n} n!\alpha^n + 1 + \sum_{n=1}^{N} \binom{N}{n} n!\alpha^n \left(\frac{N-n}{N}\right). \tag{B3}$$

But,

$$\frac{1}{\alpha N}\sum_{n=1}^{N}\binom{N}{n}n!\alpha^n=\sum_{n=1}^{N}\frac{(N-1)!}{(N-n)!}\alpha^{n-1}= \\ =\sum_{m=0}^{N-1}\frac{(N-1)!}{(N-1-m)!}\alpha^m, \tag{B4}$$

while

$$1+\sum_{n=1}^{N-1}\frac{(N-1)!}{(N-1-n)!}\alpha^n=\sum_{n=0}^{N-1}\frac{(N-1)!}{(N-1-n)!}\alpha^n, \tag{B5}$$

so that both are $S_{N-1}(\alpha)$. Thus, we arrive at a compact expression:

$$P_0=\frac{1}{2S_{N-1}(\alpha)}. \tag{B6}$$

Appendix C: Coarse-grained vorticity around a plaquette

Consider a pair of individuals, i and j, providing four states, (m_i, m_j), and the net currents around the plaquette (as in Eqn. A1). Defining $\hat{m}$ as $\vec{m}$ *without* the pair (m_i, m_j), then the persistent currents around the loop are

$$K^*(\{0,0,\hat{m}\}\to\{1,0,\hat{m}\})= \\ =\sigma(P_0/N)\,\alpha^\nu(\nu-1)!\sum_{k\neq i,j}a_i^k m_k, \tag{C1}$$

$$K^*(\{0,1,\hat{m}\}\to\{1,1,\hat{m}\})= \\ =\sigma(P_0/N)\,\alpha^{\nu+1}\nu!\left[\sum_{k\neq i,j}a_i^k m_k+a_i^j\right], \tag{C2}$$

$$K^*(\{1,0,\hat{m}\}\to\{1,1,\hat{m}\})= \\ =\sigma(P_0/N)\,\alpha^{\nu+1}\nu!\left[\sum_{k\neq i,j}a_j^k m_k+a_j^i\right], \tag{C3}$$

$$K^*(\{0,0,\hat{m}\}\to\{0,1,\hat{m}\})= \\ =\sigma(P_0/N)\,\alpha^\nu(\nu-1)!\sum_{k\neq i,j}a_j^k m_k, \tag{C4}$$

where $\nu\equiv n(0,0,\hat{m})$ is the number of infected in $\hat{m}$, and must be positive here. The $\nu=0$ case is special, as $K^*\left(\vec{0}\to\{1,0,...,0\}\right)=0$.

Now, the vorticity around this plaquette is

$$\omega_{ij}^*\equiv K(\{0,0,\hat{m}\}\to\{1,0,\hat{m}\})+ \\ +K(\{1,0,\hat{m}\}\to\{1,1,\hat{m}\})- \\ -K(\{0,1,\hat{m}\}\to\{1,1,\hat{m}\})- \\ -K(\{0,0,\hat{m}\}\to\{0,1,\hat{m}\}). \tag{C5}$$

Thus,

$$\omega_{ij}^*=\sigma(P_0/N)\,\alpha^\nu(\nu-1)!\times \\ \times\left[(\alpha\nu-1)\sum_{k\neq i,j}(a_j^k-a_i^k)m_k+2\nu\alpha a_j^i\right],$$

for $\nu>0$, and simply $2\sigma\alpha a_j^i(P_0/N)$ for $\nu=0$. To proceed further, let us define the 'coarse-grained' vorticity,

$$\omega_{ij|cg}^*\equiv\sum_{\{\hat{m}\}}\omega_{ij}^*=\hat{\omega}a_j^i, \tag{C6}$$

and find $\hat{\omega}$. First, note that, for any k,

$$\sum_{\{\hat{m}\}}m_k\delta\left(\nu-\sum_{\ell\neq i,j}m_\ell\right)= \\ =\sum_{\{\hat{m}\}}\frac{\Sigma_k m_k}{N-2}\delta(...)=\frac{\nu}{N-2}\binom{N-2}{\nu}. \tag{C7}$$

Next, note

$$0=\sum_k a_j^k=\sum_{k\neq i,j}a_j^k+a_j^i, \tag{C8}$$

and

$$\sum_{\{\hat{m}\}}=\sum_\nu\sum_{\{\hat{m}\}}\delta\left(\nu-\sum_{\ell\neq i,j}m_\ell\right). \tag{C9}$$

Thus,

$$\omega_{ij|cg}^*=\frac{2\sigma a_j^i P_0}{N}\left[\alpha+ \\ +\sum_{\nu>0}\binom{N-2}{\nu}\alpha^\nu\nu!\left[\alpha+\frac{1-\alpha\nu}{N-2}\right]\right]. \tag{C10}$$

Rewriting

$$\alpha+\frac{1-\alpha\nu}{N-2}=\frac{1}{N-2}+\alpha\frac{N-2-v}{N-2} \tag{C11}$$

and combining the last term:

$$\alpha+\sum_{\nu>0}\binom{N-2}{\nu}\alpha^\nu\nu!\left[\alpha\frac{N-2-v}{N-2}\right]= \\ =\alpha\sum_{\nu=0}^{N-3}\binom{N-3}{\nu}\alpha^\nu\nu!, \tag{C12}$$

we find

$$\hat{\omega}=\frac{\sigma}{NS_{N-1}(\alpha)}\left(\frac{S_{N-2}(\alpha)-1}{N-2}+\alpha S_{N-3}(\alpha)\right). \tag{C13}$$

Appendix D: Network Construction

The matrix a^i_j in the numerical simulations was constructed using the following algorithm:

1. begin with an all-to-all connected network
2. pick a node
3. compute the current difference, Δ, between the outgoing and incoming degrees, where an undirected edge makes no contribution to the difference
4. pick an undirected edge attached to that node
5. assign a direction to chosen edge according to the following rule: if $\Delta = 1$ make the edge incoming, if $\Delta = -1$ make the edge outgoing, if $\Delta = 0$ pick the edge direction at random
6. consider the node at the other end of that edge
7. repeat steps 3 through 6
8. arriving at a node with no undirected edges, randomly pick a node that still has undirected edges and repeat steps 2 through 7

Thus, we trace out the entire network assigning the edge directions, making sure that the current incoming and outgoing degrees of the current node are equal. In the end of this process we obtain a network where every node has equal in and out degrees.

[1] R. K. P. Zia and B. Schmittmann, Journal of Statistical Mechanics: Theory and Experiment **2007**, P07012 (2007).
[2] R. K. P. Zia and B. Schmittmann, Journal of Physics A: Mathematical and General **39**, L407 (2006).
[3] T. L. Hill, Journal of Theoretical Biology **10**, 442 (1966).
[4] J. Schnakenberg, Rev. Mod. Phys. **48**, 571 (1976).
[5] W. O. Kermack and A. G. McKendrick, Proceedings of the Royal Society, London **115** (1927).
[6] R. M. Anderson and R. M. May, *Infectious diseases of humans : dynamics and control / Roy M. Anderson and Robert M. May* (Oxford University Press Oxford ; New York, 1991).
[7] D. J. Daley, J. Gani, and J. M. Gani, *Epidemic Modelling: An Introduction*, Cambridge Studies in Mathematical Biology (Cambridge University Press, 2001).
[8] L. Allen, in *Mathematical Epidemiology*, edited by F. Brauer, P. Driessche, and J. Wu (Springer Berlin Heidelberg, 2008), vol. 1945 of *Lecture Notes in Mathematics*, pp. 81–130.
[9] R. J. Glauber, Journal of Mathematical Physics **4**, 294 (1963).
[10] D. T. Gillespie, The Journal of Physical Chemistry **81**, 2340 (1977).
[11] C. Moore and M. E. J. Newman, Phys. Rev. E **61**, 5678 (2000).
[12] R. Pastor-Satorras and A. Vespignani, Physical Review E **63**, 1 (2001).
[13] M. J. Keeling and K. T. Eames, Journal of The Royal Society Interface **2**, 295 (2005).
[14] A. Barrat, M. Barthlemy, and A. Vespignani, *Dynamical Processes on Complex Networks* (Cambridge University Press, New York, NY, USA, 2008).
[15] A. N. Kolmogorov, Math. Ann. **112**, 155 (1936).
[16] T. M. Liggett, *Interacting Particle Systems* (Springer-Verlag, New-York, 1985), 1st ed.
[17] H. Spohn, *Large scale dynamics of interacting particles* (Springer-Verlag, New-York, 1991), 1st ed.
[18] G. M. Schütz, *Exactly Solvable Models for Many-Body Systems Far from Equilibrium, Phase Transitions and Critical Phenomena vol 19* (Academic Press, San Diego, 2001), C. Domb and J. L. Lebowitz ed.
[19] F. Spitzer, Adv. in Math. **5**, 246 (1970).
[20] J. B. Weiss, B. Fox-Kemper, D. Mandal, and R. K. P. Zia, to be published in New Journal of Physics.
[21] M. Lax, Rev. Mod. Phys. **38**, 541 (1966).
[22] C. Penland and T. Magorian, Journal of Climate **6**, 1067 (1993).
[23] J. B. Weiss, Geophysical Research Letters **36**, L10705 (2009).
[24] There are many other ways to introduce infection from two or more individuals. For example, if each can infect our i independently with probability λ, then we would write $\gamma = 1 - (1 - \lambda)^n$ instead.